



Kent Academic Repository

Newport, Robert J., Penfold, J. and Williams, W.G. (1984) *Electron-Volt Spectroscopy On A Pulsed Neutron Source*. Nuclear Instruments and Methods in Physics Research, 224 (1-2). pp. 120-132. ISSN 0168-9002.

Downloaded from

<https://kar.kent.ac.uk/15939/> The University of Kent's Academic Repository KAR

The version of record is available from

[https://doi.org/10.1016/0167-5087\(84\)90456-3](https://doi.org/10.1016/0167-5087(84)90456-3)

This document version

UNSPECIFIED

DOI for this version

Licence for this version

UNSPECIFIED

Additional information

Versions of research works

Versions of Record

If this version is the version of record, it is the same as the published version available on the publisher's web site. Cite as the published version.

Author Accepted Manuscripts

If this document is identified as the Author Accepted Manuscript it is the version after peer review but before type setting, copy editing or publisher branding. Cite as Surname, Initial. (Year) 'Title of article'. To be published in *Title of Journal*, Volume and issue numbers [peer-reviewed accepted version]. Available at: DOI or URL (Accessed: date).

Enquiries

If you have questions about this document contact ResearchSupport@kent.ac.uk. Please include the URL of the record in KAR. If you believe that your, or a third party's rights have been compromised through this document please see our [Take Down policy](https://www.kent.ac.uk/guides/kar-the-kent-academic-repository#policies) (available from <https://www.kent.ac.uk/guides/kar-the-kent-academic-repository#policies>).

ELECTRON VOLT SPECTROSCOPY ON A PULSED NEUTRON SOURCE

R.J. NEWPORT, J. PENFOLD and W.G. WILLIAMS

*Neutron Division, Rutherford Appleton Laboratory,
Chilton, Didcot, Oxon, OX11 0QX, England*

Received 18 November 1983 and in revised form 10 January 1984

The principal design aspects of a pulsed source neutron spectrometer in which the scattered neutron energy is determined by a resonance absorption filter difference method are discussed. Calculations of the accessible dynamic range, resolution and spectrum simulations are given for the spectrometer on a high intensity pulsed neutron source, such as the spallation neutron source (SNS) now being constructed at the Rutherford Appleton Laboratory. Special emphasis is made of the advantage gained by placing coarse and fixed energy-sensitive filters before and after the scatterer; these enhance the inelastic/elastic discrimination of the method. A brief description is given of a double difference filter method which gives a superior difference peak shape, as well as a better energy transfer resolution. Finally, some first results of scattering from zirconium hydride, obtained on a test spectrometer, are presented.

1. Introduction

The special characteristic of the new pulsed neutron sources is their relatively high flux of epithermal neutrons, and for inelastic scattering this offers the potential of condensed matter research in previously inaccessible regions of (Q, ω) space. There is in particular now the prospect of exploiting this property to measure energy transfers in the eV region [1]. A prerequisite for this, however, is the need to develop spectrometers having efficient monochromators and detectors at neutron energies $E \sim 1$ eV. This paper describes one method of using nuclear resonance absorption as a means of energy selection in inelastic time-of-flight spectrometers.

One of the important criteria required of the designed spectrometer was the ability to able to measure eV energy transfers (eg. $\hbar\omega > 0.5$ eV) with low associated momentum transfers ($\hbar Q < 4 \text{ \AA}^{-1}$). This is an area of experimental materials physics which has not hitherto been accessible, and it is one of considerable interest as illustrated by the following examples:

(a) The study of high energy vibrational modes in solids requires low values of Q to reduce multiphonon scattering. Multiphonon contributions may influence both the position and the widths of observed inelastic peaks.

(b) Measurements of high frequency molecular vibration in liquid or gaseous samples require low Q values to minimise the effect of diffusional broadening.

(c) In measuring magnetic excitations the scattering cross-section is modulated by the square of the magnetic form factor $F(Q)$. These functions are approximately Gaussian with half-heights occurring in the range

$3-5 \text{ \AA}^{-1}$. In view of the fact that the intensity of magnetically scattered neutrons are reduced to a quarter of their maximum values at these Q 's, it is evident that the lowest possible Q values are needed for magnetic scattering experiments.

(d) As a corollary to the more general magnetic scattering cases there has been a recent theoretical study [2] of the potential use of inelastic neutron scattering as a means of examining the single particle excitation of electrons across the band gap in semiconductors. Such an experiment, if possible, would provide information on non- k -conserving transitions and in particular on conduction-band structure; it would therefore represent a valuable addition to existing optical methods.

There are two basic methods of using nuclear absorption resonances in eV neutron spectroscopy. The first is the resonance detector spectrometer [3-6] where the absorbing foil in the scattered beam captures neutrons within the resonance energy width and a scintillation detector registers the resulting gamma ray cascade. This is an example of the inverse geometry class of pulsed source inelastic instruments. The second method is a difference technique using neutron detectors, commonly called the filtered beam spectrometer [7-10], where the energy-sensitive absorber is placed either in the incident (direct geometry) or in the scattered beam (see fig. 1). The difference neutron time-of-flight spectra collected with and without the resonance absorber then give either the sample's response to the resonance energy incident neutrons, or, in the inverse geometry case, identify those neutrons scattered to the resonance energy. In this paper we argue that the inverse geometry is generally the better one for nuclear resonance energy

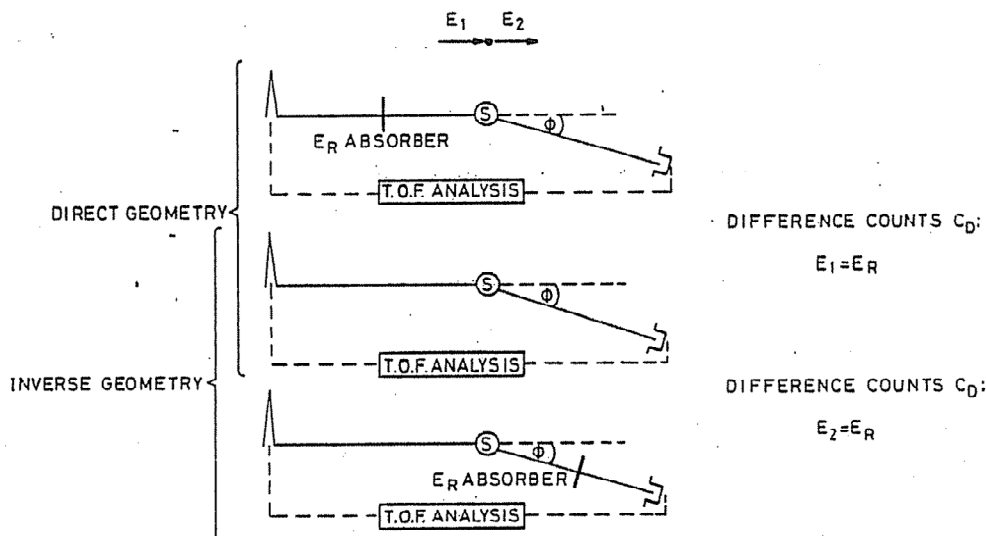


Fig. 1. Principle of resonance filter difference method in direct and inverse geometries.

selectors, and have designed and constructed a filter difference spectrometer which uses resonance foil analysers and neutron detectors. The spectrometer is technically simpler to construct than the resonance detector spectrometer.

Since one of the main aims of this work was to investigate the possibility of using the difference technique to measure low Q scattering processes, it was essential to design the spectrometer with detectors at the lowest possible scattering angles ϕ . It is the ability to measure scattering at small ϕ values which is likely to be the major limiting factor in achieving very low Q values ($Q \leq 2 \text{ \AA}^{-1}$). The measurements presented in this paper show that we have succeeded in measuring difference spectra down to a scattering angle $\phi = 5^\circ$. We give the first results of low Q measurements for a zirconium hydride scatterer using the resonance absorber difference principle (see ref. [8]); similar measurements have been reported by the Los Alamos Group [11].

2. Spectrometer resolutions

The energy widths of nuclear resonance peaks ΔE_R are generally of the order 0.1 eV, which is typically 10–50% of the energy transfers to be measured. This width dominates both the energy and momentum transfers, at least for $\hbar\omega$ up to 1 eV. The energy transfer resolutions due to this width for direct (D) and inverse (I) geometry spectrometers are given by:

$$\left[\frac{\Delta \hbar\omega}{\hbar\omega} \right]_I = \frac{\Delta E_R}{\hbar\omega} \left[1 + \frac{L_{2I}}{L_{1I}} \left(\frac{E_1}{E_R} \right)^{1.5} \right] \quad (1)$$

$$\left[\frac{\Delta \hbar\omega}{\hbar\omega} \right]_D = \frac{\Delta E_R}{\hbar\omega} \left[1 + \frac{L_{1D}}{L_{2D}} \left(\frac{E_2}{E_R} \right)^{1.5} \right] \quad (2)$$

where E_R is the resonance energy, E_1 and E_2 are the incident and scattered neutron energies and L_1 and L_2 and the incident and scattered beam flight paths.

It is instructive to compare the performance of the direct and inverse geometry spectrometers by calculating these resolution terms for instrument geometrical parameters where the difference count rates (per unit energy transfer) are equated. By matching the incident and scattered beam solid angles and assuming equal source and detector areas we obtain equivalent count rates with:

$$L_{1D}L_{2D} = L_{1I}L_{2I} \quad (3)$$

The energy resolution equations require $L_{2I} \ll L_{1I}$ and $L_{2D} \gg L_{1D}$ on pulsed neutron sources the first condition is relatively easily satisfied, the second, however, is not. For the SNS L_{1D} must be greater than about 6 m since the source requires extensive biological shielding out to this distance. Fig. 2 shows these energy resolution terms for the following hypothetical (but practical) spectrometer geometries with count rate equivalence:

$$\begin{aligned} L_{1D} &= 6 \text{ m}, & L_{2D} &= 3 \text{ m}, \\ L_{1I} &= 18 \text{ m}, & L_{2I} &= 1 \text{ m}, \\ E_R &= 1 \text{ eV}, & \Delta E_R &= 0.1 \text{ eV}. \end{aligned}$$

These curves show conclusively that the inverse geometry arrangement gives the better energy resolution, and in the remainder of this paper we restrict ourselves to a fuller consideration of eV difference spectrometers which

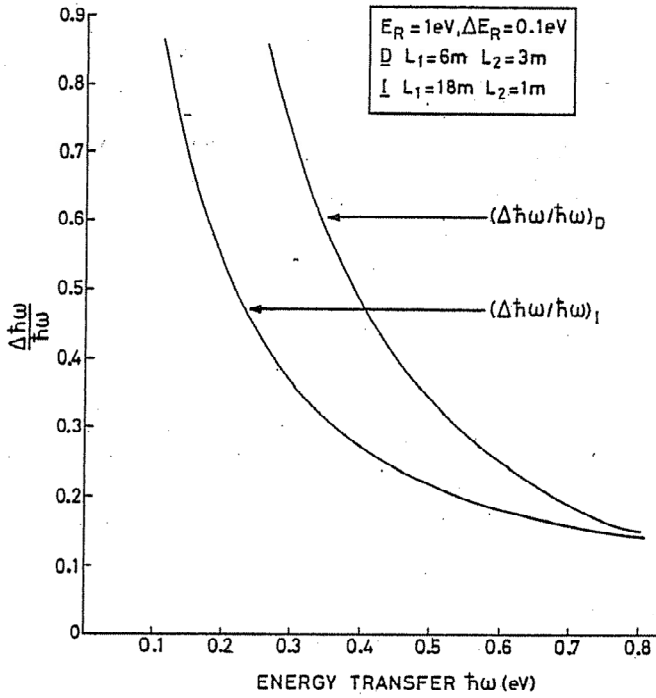


Fig. 2. Energy transfer resolutions in direct and indirect geometries.

use nuclear resonance analysers placed in the scattered beam.

The complete formulae for the energy and momentum transfer resolutions of inverse geometry instruments have been derived by Richardson [12] and are applied in the following to nuclear resonance analysers. The resultant fwhm values associated with $\hbar\omega$ and Q are:

$$\Delta(\hbar\omega) = \left\{ \left[1 + \left(\frac{E_1}{E_R} \right)^{1.5} \frac{L_2}{L_1} \right]^2 \Delta^2(E_R) + \left[\frac{2E_1^{1.5}}{AL_1} \right]^2 \Delta^2(t) + \left[\frac{2E_1^{1.5}}{L_1 E_R^{0.5}} \right]^2 \Delta^2(L_2) + \left[\frac{2E_1}{L_1} \right]^2 \Delta^2(L_1) \right\}^{0.5}, \quad (4)$$

$$\Delta(Q) = \frac{B^2}{2Q} \left\{ \left[1 - \left(\frac{E_1}{E_R} \right)^{1.5} \frac{L_2}{L_1} - \cos\phi \left[\left(\frac{E_1}{E_R} \right)^{0.5} - \frac{L_2}{L_1} \frac{E_1}{E_R} \right] \right]^2 \Delta^2(E_R) + \left[\frac{2E_1^{1.5}}{AL_1} \right]^2 \Delta^2(t) + \left[\frac{2E_1^{1.5}}{L_1 E_R^{1.5}} \right]^2 \Delta^2(L_2) \right\}^{0.5}$$

$$+ \left(\frac{2E_1}{L_1} \right) \Delta^2(L_1) \left\{ \left[\left(\frac{E_R}{E_1} \right)^{0.5} \cos\phi - 1 \right]^2 + \left[2(E_1 E_R)^{0.5} \sin\phi \right]^2 \Delta^2(\phi) \right\}^{0.5} \quad (5)$$

where $\Delta(L)$, $\Delta(E)$ etc. are fwhm values of the appropriate energy and length distributions, ϕ is the scattering angle, t is the total time-of-flight, and A and B are constants equal to $72.3 \text{ eV}^{0.5} \mu\text{s m}^{-1}$ and $21.97 \text{ \AA}^{-1} \text{ eV}^{-0.5}$ respectively. These equations are used in section 6 to calculate the resolutions of typical inverse geometry spectrometers with $\text{Sm}(E_R = 0.872 \text{ eV})$ and $\text{Ta}(E_R = 4.28 \text{ eV})$ analysers.

3. Nuclear resonance analysers

The reaction cross-section in the vicinity of a well-separated resonance peak occurring in the eV region can be described by a single level, s-wave dispersion formula [13,14] usually referred to as the Breit-Wigner expression:

$$\sigma(E) = \frac{\sigma_0}{1 + 4(E - E_R)/\Gamma^2}, \quad (6)$$

where σ_0 is the cross-section at $E = E_R$ (suitably weighted for isotopic abundance).

For the isotopes considered here the total resonance width Γ is given by the sum of the gamma radiative and neutron widths:

$$\Gamma = \Gamma_\gamma + \Gamma_n. \quad (9)$$

For the narrowest nuclear resonances of interest in this paper it is essential to include the Doppler broadening Δ_D in the cross-section width function. This effect has been treated in detail elsewhere [13,15], however, to first order it approximates to an effective resonance width $(\Gamma + \Delta_D)$ and a peak cross-section $\Gamma\sigma_0/(\Gamma + \Delta_D)$ with

$$\Delta_D = (4k_B T E_R / M)^{0.5}, \quad (10)$$

where k_B is Boltzmann's constant, T is the absolute temperature and M is the nuclear mass.

The most useful nuclear resonance analysers are those having a high σ_0 (for sensitivity) and a low effective width $(\Gamma + \Delta_D)$ (for resolution). The resonance should also be well separated from other significant higher energy resonances. The off-resonance cross-section should be low compared to σ_0 . Table 1 shows some of the nuclear resonances which could be utilised in a filter difference spectrometer. Plutonium isotopes have fabrication and handling problems and have not been seriously considered for use at this stage. Antimony and uranium have very high E_R values and are not suitable

Table 1
Potentially useful resonances for filter difference method

Isotope	Natural abundance	E_R (eV)	Γ (meV)	Δ_{D293} (meV)	σ_0 (b)	Next higher resonance (eV)
^{149}Sm	0.138	0.872	61	25	20700	3.4 (^{147}Sm)
^{240}Pu	—	1.056	33	21	172000	20.5
^{242}Pu	—	2.67	27	34	73000	54.0
^{181}Ta	1.0	4.28	57	50	23800	10.3
^{121}Sb	0.573	6.24	90	73	4960	15.5
^{238}U	0.993	6.67	28	54	21800	21.0

first test candidates for low Q work since they require detection angles $\phi \sim 1^\circ$. Samarium is potentially very useful in that it is possible to polarise the nucleus [16] and this allows the possibility of later extending the basic method to look at spin-dependent scattering processes. The tantalum resonance allows energy transfers up to 1 eV to be observed with momentum transfers below 5 \AA^{-1} at a scattering angle $\sim 2^\circ$. We shall show that the resonance energies of Sm and Ta are at convenient values to enable an energy-selective course filter technique to be applied which greatly improves the inelastic scattering/elastic scattering discrimination of the filter difference method. Sm and Ta were therefore chosen as the most suitable resonance analysers for test measurements and further discussion in this paper will be restricted to their use.

The optimum resolutions and difference count rates in the spectrometer depend on an optimisation of the thickness of the resonance analyser. Clearly if the analyser foil is excessively thin the IN/OUT difference counts will fall below the optimum level, whereas very thick foils degrade the instrument resolution. The difference counts are proportional to the attenuation profile across the resonance which is given by:

$$A(E) = 1 - \exp(-\sigma Nd), \quad (11)$$

where N is the nuclear density of the absorber and d the analyser thickness (which clearly must be very uniform). The energy dependence of σ is taken as implicit and the functional labelling (E) will be omitted in the remainder of the paper.

The optimum foil thickness for a given resonance absorber at a given temperature must then be determined, using some quality factor. Due to lack of experience with these spectrometers it is not clear at present which criteria should be set to define this quality factor. Seeger et al. [10] have recently considered this problem in some detail, and have proposed a quality factor based on the statistical variation of counts across the complete attenuation peak. In this work, however, we have used a somewhat simpler approach which is similar to that used in triple axis neutron spectroscopy [17]. We define the quality factor as

$$C_R = A(E_R)/\Delta^2 E_R, \quad (12)$$

where $A(E_R)$ is the peak attenuation factor and ΔE_R is the fwhm of the attenuation peak. The optimum analyser thickness obtained using this method for the Sm and Ta resonance absorbers are shown in table 2 under the "thin" foil column. Temperature dependent effects on the resonance absorption peak were evaluated as discussed above.

4. Coarse energy filters

The major disadvantage of difference techniques is the statistical problem arising from the subtraction of two large numbers. This difficulty can be considerably reduced in resonance filter spectrometers designed to look at inelastic scattering by (1) removing resonance energy neutrons from the incident beam and (2) selec-

Table 2
Optimised analyser thicknesses in single and double difference experiments

Analyser	"Thin" foil					"Thick" foil			Double difference		C_{DD}
	Temp. (K)	Nd (at. cm^{-2})	d (mm)	$A(E_R)$	ΔE_R (meV)	Temp. (K)	Nd (at. cm^{-2})	d (mm)	$DD(E_R)$	ΔE_R (meV)	
^{149}Sm	293	6.0×10^{20}	0.23	0.74	100	293	37.4×10^{20}	1.25	0.55	81	1.14
	77	5.7×10^{20}	0.19	0.71	88	293	27.4×10^{20}	0.91	0.50	68	1.17
^{181}Ta	293	1.2×10^{20}	0.022	0.77	134	293	7.1×10^{20}	0.13	0.61	116	1.04
	77	0.9×10^{20}	0.05	0.73	100	293	4.2×10^{20}	0.075	0.53	82	1.09

tively attenuating neutrons at energies $E > E_R$ in the scattered beam which are elastically scattered by the sample. In our spectrometer design this is achieved by using two stationary energy-sensitive filters.

The purpose of the incident beam filter is to selectively attenuate neutrons of energies up to E_R . The two most important components are a thick layer of the resonance material itself and a low energy absorber such as cadmium. The resonance absorber ensures that no $E = E_R$ neutrons are incident at the scatterer. Thus, any E_R neutrons detected by the difference method must have been inelastically scattered. The thermal neutron absorber serves not only to reduce general neutron background but also to remove frame overlap slow neutrons. It is also advantageous to remove as many neutrons with energies between the Cd resonance and E_R so to further reduce background levels. These ideal requirements can only be fully realised using static

resonance filters in the Sm foil analyser case; here a combination of Cd ($E_R = 0.178$ eV), Er ($E_R = 0.46$ and 0.584 eV) and Sm ($E_R = 0.098$ and 0.873 eV) filters provides low transmittances at all energies almost up to ~ 1 eV (fig. 3). Corresponding filter combinations are not available for the Ta analyser, though here it is still desirable to have the same good absorption up to ~ 1 eV as well as a thick tantalum absorber in the incident beam.

The second filter assembly (filter B) is placed in the scattered beam to reduce the counts detected due to elastic scattering at energies just above E_R (since these may fall within the time channels associated with the inelastic events of interest). In the Sm foil analyser case this is accomplished using a combination of Hf (1.098 eV), Rh (1.257 eV) and In (1.457 eV) resonance filters (fig. 3). For the Ta analyser it is possible to use Au (4.906 eV) and Ag (5.19 eV) resonances to perform the

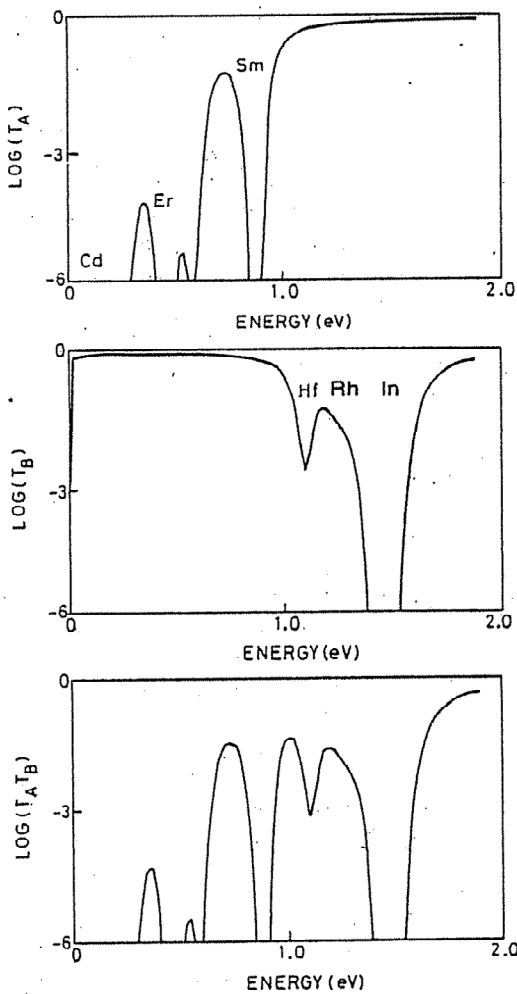


Fig. 3. Transmittances of the incident (A) and scattered (B) beam filters - samarium case.

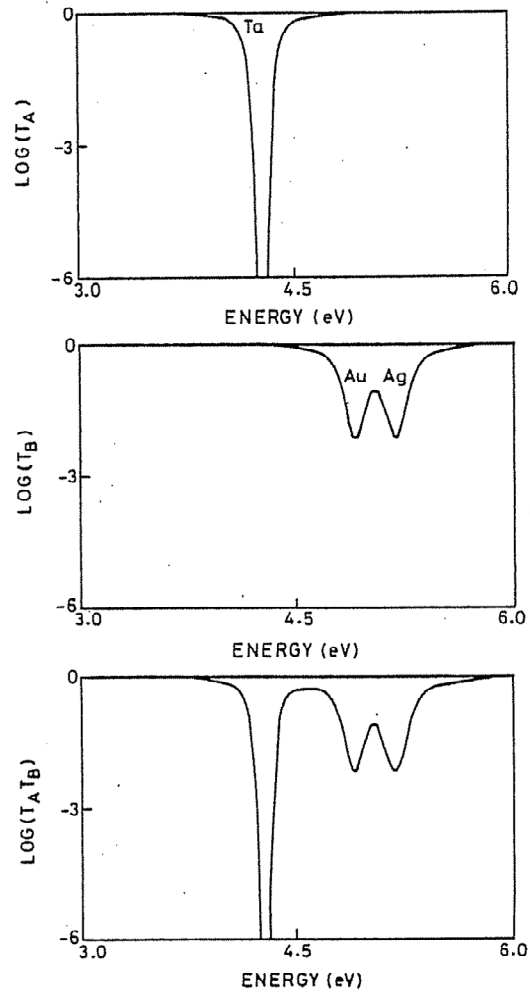


Fig. 4. Transmittances of the incident (A) and scattered (B) beam filters - tantalum case.

Table 3
Incident and scattered beam filters

Analyser	Fixed filters	Material	Resonances used (eV)	$Nd(10^{21} \text{ at. cm}^{-2})$	$d(\text{mm})$
Sm	incident beam	Cd	0.178	9.3	2.0
		Er_2O_3 (powder)	0.46, 0.58	10.0 (Er)	15.0
		Sm_2O_3 (powder)	0.098, 0.872	9.2 (Sm)	30.0
	scattered beam	In	1.46	19.0	0.5
		Rh	1.26	3.6	0.25
		Hf	1.1	11.0	0.25
Ta	incident beam	Ta	1.1	14.0	0.25
	scattered beam	Ag	5.19	4.1	0.07
		Au	4.91	1.6	0.027

same function (fig. 4). The characteristics of the incident and scattered beam filters chosen for the Sm and Ta analyser experiments are listed in table 3.

It is worth reiterating that the purpose of these filters is to reduce the number of counts collected in the time bins where a difference count due to inelastic scattering

can be expected: they improve the sensitivity of the difference method but do not contribute to the difference count. The transmittance product $T_A T_B$ for elastic scattering produces a constant "baseline" count in the two parts of the difference measurement. The inelastic difference counts themselves are proportional to $T_A T_B$, where T_A is now the incident filter transmittance at a neutron energy ($E_R + \hbar\omega$) and T_B that of the fixed scattered beam filter at the resonance energy E_R . Fig. 5 shows this product for both the Sm and Ta analysers. Elastic-inelastic discrimination by this method will only generally be useful for transmittance products ≥ 0.1 since smaller values give an unacceptable reduction in the difference count rates. In practice this means that the static filtering technique becomes less effective for energy transfers less than ~ 0.2 eV.

5. Double difference method

The attenuation function across a resonance absorption peak as given by eq. (11) is Lorentzian. The extensive wings in a single peak difference count can become problematic in a spectrum where there is considerable peak overlap and the double difference technique, as first proposed by Seeger [10] offers a method for minimising this effect. Expansion of eq. (6) around $E = E_R$ shows that (1) the wings of the peak fall off in proportion to $(E - E_R)^{-2}$ and (2) that the function has no second moment and therefore no well-defined variance. Seeger suggested using two analysing foils: a "thin" foil where $Nd = \alpha$ and a "thick" foil of the same type as the first but with a nuclear thickness $Nd = \alpha/\beta$ where $\beta < 1$. The functional form of the wings of the two attenuations scale linearly with thickness. It is therefore possible, in principle, to eliminate much of the wing problem inherent in the single difference method by differencing thick and thin foil measurements, the counts for the

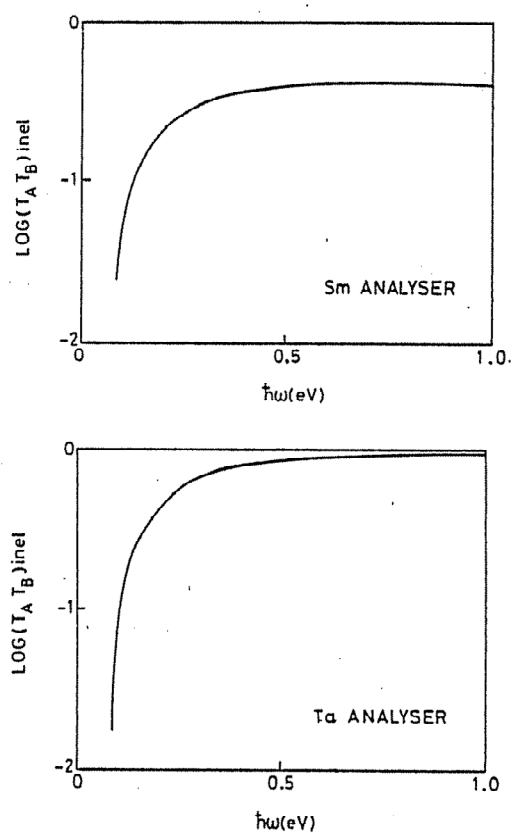


Fig. 5. Inelastic scattering discrimination provided by the incident and scattered beam filters.

thick foil being multiplied by β to bring the asymptotic level to the same value as that for the thin foil counts. Normalising to the foil out counts N_0 , the double difference counts at the resonance energy are given by:

$$DD(E_R) = N_0 \{ 1 - \exp(-\sigma_0 \alpha) - \beta [1 - \exp(-\sigma_0 \alpha / \beta)] \}. \quad (13)$$

By expanding this function around E_R it can be shown that the double difference counts fall off very rapidly away from E_R in comparison with the single difference case. The double difference function has a finite second moment and a much narrower fwhm.

We have examined the possibility of applying the double difference method to the Sm and Ta analysers. The first requirement is to choose the best α and β combinations for different experimental conditions. Seegar et al. [10] have recently addressed this problem in some detail. In the present work we have, for consistency reasons, continued to use a more empirical double difference quality factor C_{DD} , analogous to that used for the single difference case. This is defined as:

$$C_{DD} = DD(E_R) / \Delta^2 E_R, \quad (14)$$

where $DD(E_R) = A(E_R)_{\text{thin}} - \beta A(E_R)_{\text{thick}}$. The optimum analyser foil thickness for the single difference method was used as the initial estimate for the "thin" foil thickness. Double difference quality factors were then determined for a series of β values, and the optimum β value found from the maxima of the C_{DD} vs. β plots. The validity of using the single difference optimum thickness for the "thin" foil was confirmed by fixing β at its optimum value and varying α around its initial value; this gave no improvement in C_{DD} . Some results for the Sm and Ta analysers are shown in table 2; some of the improvement arising from the double difference procedure is indicated in the quality factor ratio (C_{DD}/C_D) thought there is in addition a much improved peak shape. There are two further advantages to be gained by employing the double difference technique. The first arises when coarse energy filters are used to improve the inelastic/elastic discrimination. In section 4 we showed that it is not possible to obtain 'perfect' discriminating filters which have constant attenuations over the large energy range of interest and there may in practice be some "leakage" of elastic as well as inelastic difference intensities in a difference spectrum at those energies where the attenuation of the discrimination filters decreases. The elastic difference intensities also scale linearly with analyser thickness if they are at energies in the higher energy wing of the main analyser resonance, consequently a weighted double difference essentially removes this leakage effect.

A second advantage arises when it is necessary to place the analysing foil in the main beam transmitted through the scattering sample. This is not an ideal geometry since a single difference measurement may

reveal analyser diffraction and self-shielding effects. However, it is evident, at least to within second order effects like multiple scattering, that these features cancel out in the weighted double difference spectrum.

6. Description of resonance analyser difference spectrometer

On the basis of the previous discussion the basic spectrometer design shown in fig. 6 was adopted for a prototype spectrometer using Sm and Ta resonance analysers, and its principle of operation is conveniently illustrated in the distance-time diagram. The detectors used in the prototype spectrometer were placed at scattering angles $\phi = 5^\circ, 10^\circ$ and 20° ; this gives the spectrometer some low Q capability. The important characteristics of the spectrometer to the materials scientist are (a) its $\hbar\omega$ and Q resolutions, (b) the dynamic range in (Q, ω) accessed by the spectrometer, and (c) the intensities. These are now discussed.

6.1. Energy and momentum transfer resolutions

The $\hbar\omega$ and Q resolutions for the resonance filter difference spectrometer were calculated using eqs. (4) and (5). Values for E_R and $\Delta(E_R)$ were taken from table 2 assuming a double difference experiment with the thin foil cooled to 77 K, i.e. $E_R = 0.872$ eV and $\Delta(E_R) = 0.068$ eV for Sm; $E_R = 4.28$ eV and $\Delta(E_R) = 0.082$ eV for Ta. The fwhm of the timing uncertainties is a combination of three terms on the SNS source: the proton pulse duration ($t_p \sim 0.4 \mu\text{s}$), the time structure during moderation ($t_M \sim 2/E_1^{0.5} \mu\text{s}$, with E_1 in units of eV), and the inherent time spread during detection ($t_d \sim 0.5 \mu\text{s}$). This yields effective ΔT values $\sim 1.6 \mu\text{s}$ for down-scattering from $E_1 = 2$ eV (which is typical for the Sm analyser) and $\sim 1.1 \mu\text{s}$ for down-scattering from $E_1 = 5$ eV (appropriate for Ta analyser). In all the calculations the incident and scattered beam flight paths and distributions were taken to be $L_1 = 10.0 \pm 0.02$ m and $L_2 = 1.0 \pm 0.02$ m respectively. These length uncertainties are approximate estimates, however their contributions to the overall resolutions are small and this does not affect the main conclusions presented. The 10 m incident flight path was chosen as a compromise to give reasonable intensities at the scatterer and suitably small collimation angles appropriate for low Q studies; $(L_2/L_1) \sim 0.1$ gives good $\hbar\omega$ resolution in the inverse geometry [eq. (4)] as well as acceptable scattered beam solid angles.

The accurate determination of detector angle and associated scattering angle distribution for 'long' proportional counters requires a detailed analysis. The value of ϕ and its distribution $\Delta\phi$ contributes to several terms in ΔQ and its weighted average must be obtained as

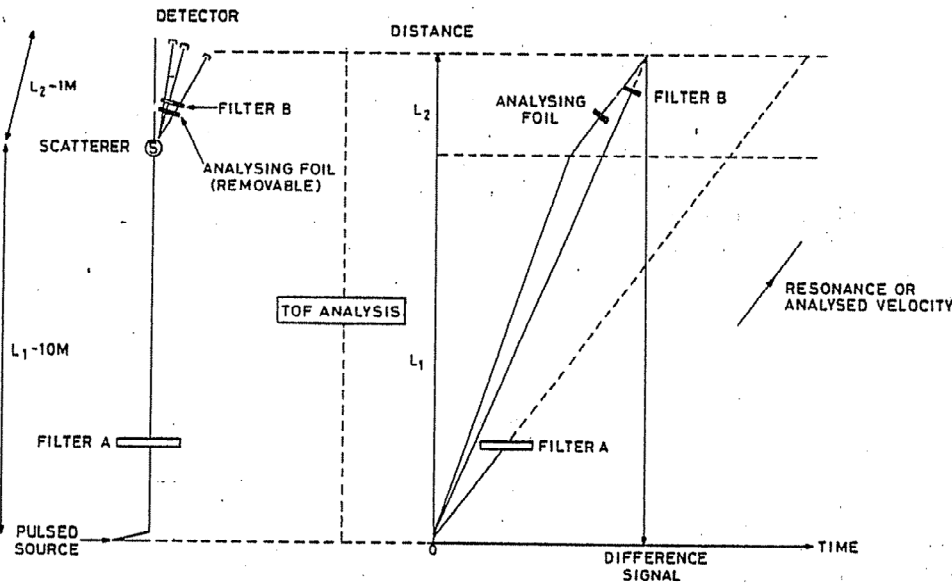


Fig. 6. Schematic diagram of the resonance foil difference method and the principle of the method in inverse geometry.

accurately as possible. A full discussion of this problem has been reported [18]. For geometric detector angles of 5° , 10° and 20° and with the assumption that all detectors are 25.4 mm diameter and have active lengths of 150 mm (5°) and 250 mm (10° , 20°), the following values of ϕ and $\Delta\phi$ were calculated for the prototype spectrometer:

- 5° : $5.54^\circ \pm 1.76^\circ$;
- 10° : $10.71^\circ \pm 2.22^\circ$;
- 20° : $20.41^\circ \pm 1.48^\circ$.

The calculated energy and momentum transfer resolutions are plotted, as a function of $\hbar\omega$, for both Sm and Ta analysers in figs. 7-10. Partial contributions are shown for the 5° detector and these curves clearly demonstrate the overall dominance of the ΔE_R term in determining both the energy and momentum transfer resolutions, at least for $\hbar\omega$ values up to ~ 1 eV.

6.2 Dynamic range (Q, ω)

Fig. 11 shows the regions of (Q, ω) space accessible using Sm and Ta resonance analysers at energies $E_R = 0.872$ eV and $E_R = 4.28$ eV respectively, and at various scattering angles. The widths of the (Q, ω) bands were calculated using the method described in section 2 and are drawn as $\pm\sigma$ widths, i.e. in terms of the standard deviations in Q and ω rather than their fwhm values. The figure demonstrates that in order to measure high energy transfers at low Q it is not only important to have high E_R values (i.e. eV energy neutrons), but it is also essential to have the ability to measure at very

small scattering angles with low background. In fact the figure illustrates that if measurements cannot be made at scattering angles $\phi < 5^\circ$ (due to a high background

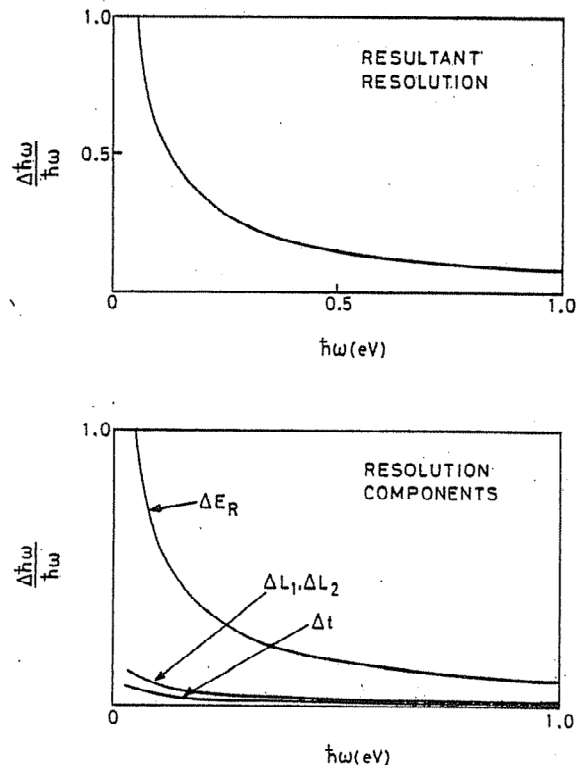


Fig. 7. Energy transfer resolution for the samarium foil double difference.

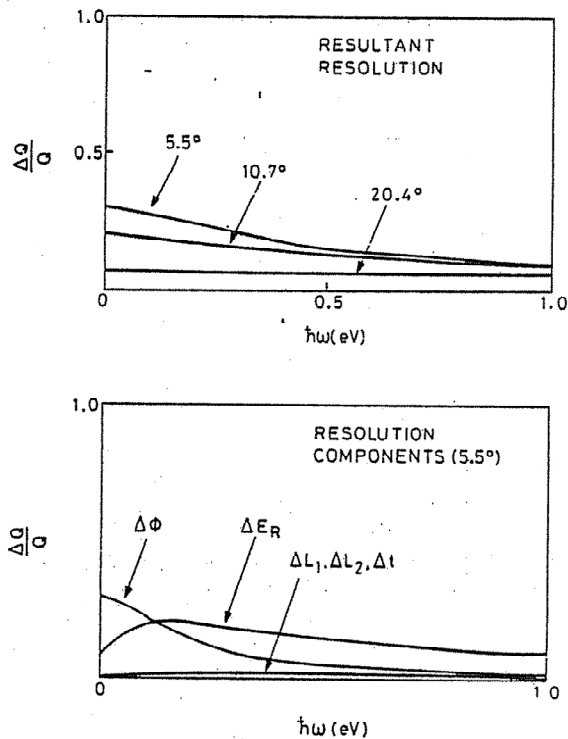


Fig. 8. Momentum transfer resolution for the samarium foil double difference.

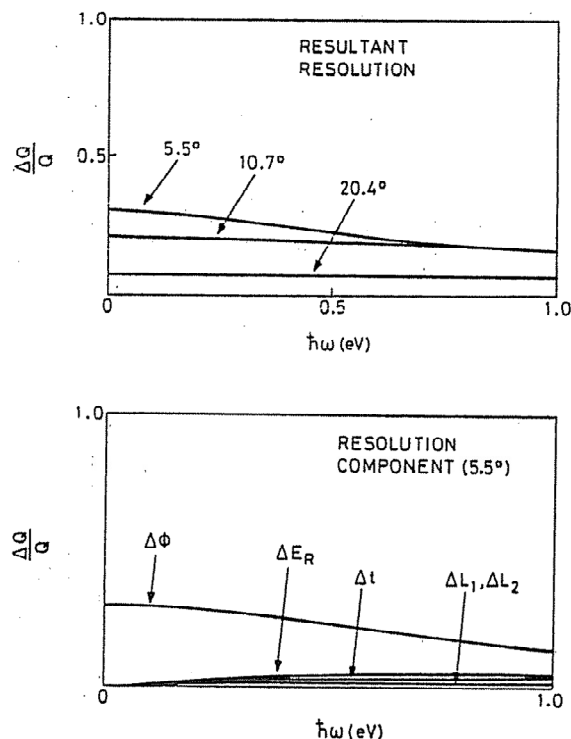


Fig. 10. Momentum transfer resolution for the tantalum foil double difference.

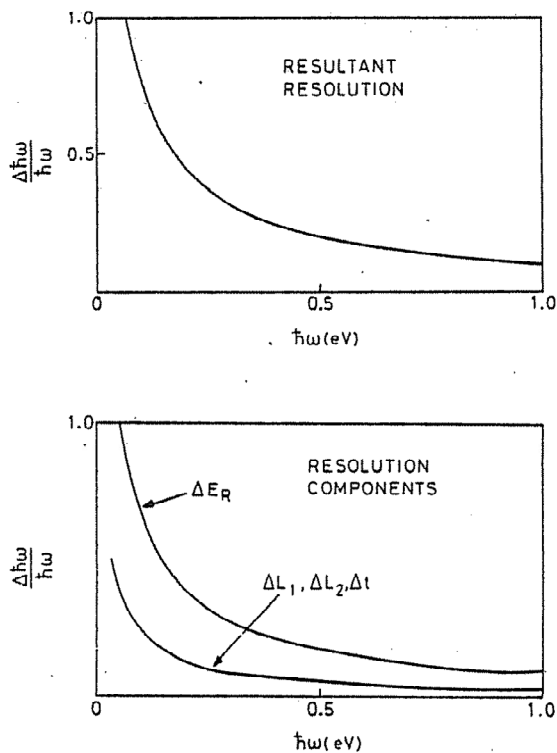


Fig. 9. Energy transfer resolution for the tantalum foil double difference.

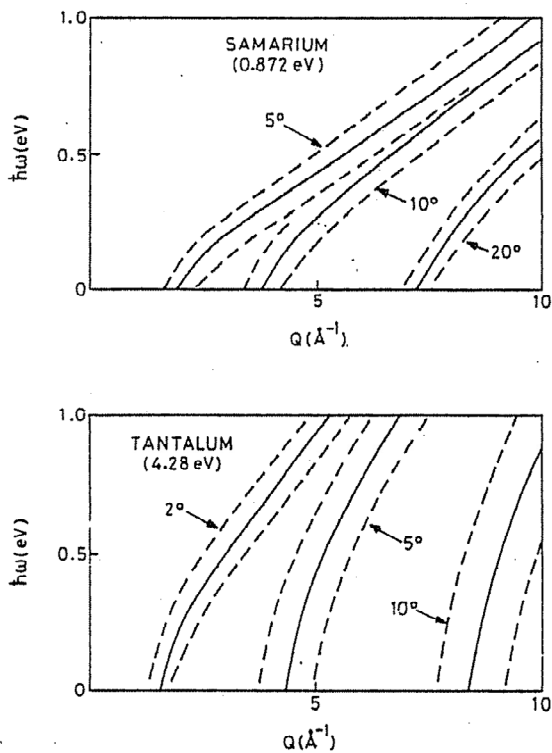


Fig. 11. Dynamic range covered by samarium and tantalum analysers at various scattering angles.

for example) then smaller Q values are achieved with the lower energy analyser (Sm). Current experience suggests that it is the small ϕ requirement which is likely to be the limiting factor in determining the effectiveness of eV spectrometer designs.

6.3. Intensity estimates

Calculations of the count rates (difference counts per second per resolution element) were made for the filter difference technique based on the method used by Richardson [12] for a beryllium filter analyser spectrometer. For a thin sample the count rate is given by:

$$I = n(E_1) A_m \frac{A_s}{L_1^2} f_s \left(\frac{E_R}{E_1} \right)^{0.5} S(Q, \omega) \times \frac{A_d}{4\pi L_2^2} \eta(E_R) T_A T_B (1 - T_R) \Delta(h\omega), \quad (15)$$

where A_m , A_s and A_d are the areas of the moderator, sample and detector respectively. The fraction of the incident beam scattered by the sample is f_s and $(E_R/E_1)^{0.5}$ is the flux factor associated with the sample's scattering cross-section. The detector efficiency is denoted by $\eta(E_R)$; this represents a mean value across the resonance peak and must be written $\eta(E)$ when a full simulation, which includes elastic scattering effects, is required. $n(E_1)$ is the number of neutrons ($\text{cm}^{-2} \text{sr}^{-1} \text{eV}^{-1} \text{s}^{-1}$) leaving the moderator face. T_A , T_B and T_R are the transmittances of the incident beam, scattered beam and analysing filters respectively and are functions of the incident and scattered neutron energies. Taking the SNS ambient moderator as the source, the

flux term can be represented as the sum of a Maxwellian, an epithermal component and a joining function $\phi(E_1)$ [19,20], where

$$F(E_1) = n(E_1) A_m = 10^{13} [3125 E_1 \exp(-E_1/0.04) + \phi(E_1) E_1^{-0.9}], \quad (16)$$

(in $\text{n eV}^{-1} \text{sr}^{-1} \text{s}^{-1}$) and

$$\phi(E_1) \sim [1 + \exp(4.708 E_1^{0.5} - 11.05)]^{-1}, \quad (17)$$

with E_1 expressed in eV. For incident neutron energies > 1 eV this expression simplifies to:

$$F(E_1) \sim \frac{7 \times 10^{12}}{E_1^{0.9}} \quad (\text{n eV}^{-1} \text{sr}^{-1} \text{s}^{-1}). \quad (18)$$

The scattering law that we have used to simulate the filter difference time-of-flight spectra is that of a unit mass Einstein oscillator. The details of the scattering law are described in ref. [12]. In practice this law is followed closely by hydrogen-metal scatterers, and we have used zirconium hydride as the test scatterer in our experiments; the fundamental frequency $\hbar\omega_0 \sim 140$ meV. The intrinsic widths of the ZrH_2 inelastic peaks are much smaller than the spectrometer resolution ($\Delta\hbar\omega \sim 0.07$ – 0.1 eV), e.g. typical intrinsic widths ~ 0.022 eV have been measured at $Q = 3.6 \text{ \AA}^{-1}$ [21], so it provides a useful test sample.

The simulated time-of-flight spectra for the fundamental and overtone peaks of an oscillator with $\hbar\omega_0 = 140$ meV are shown in figs. 12 and 13 for Sm and Ta analysers respectively. We show for comparison curves calculated for both the single and double difference

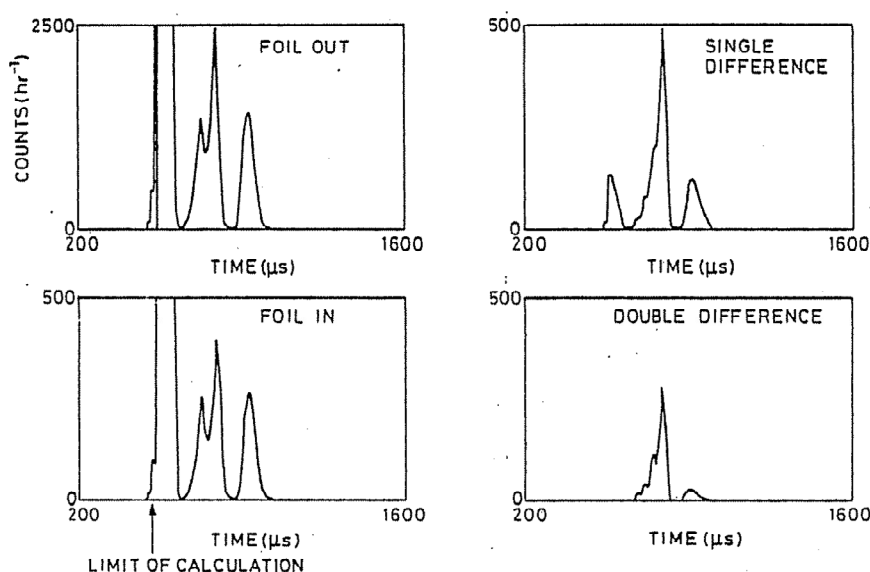


Fig. 12. Simulated TOF spectra for a 25% zirconium hydride scatterer on the prototype eVS at full SNS intensity ($\phi = 5^\circ$); samarium analyser.

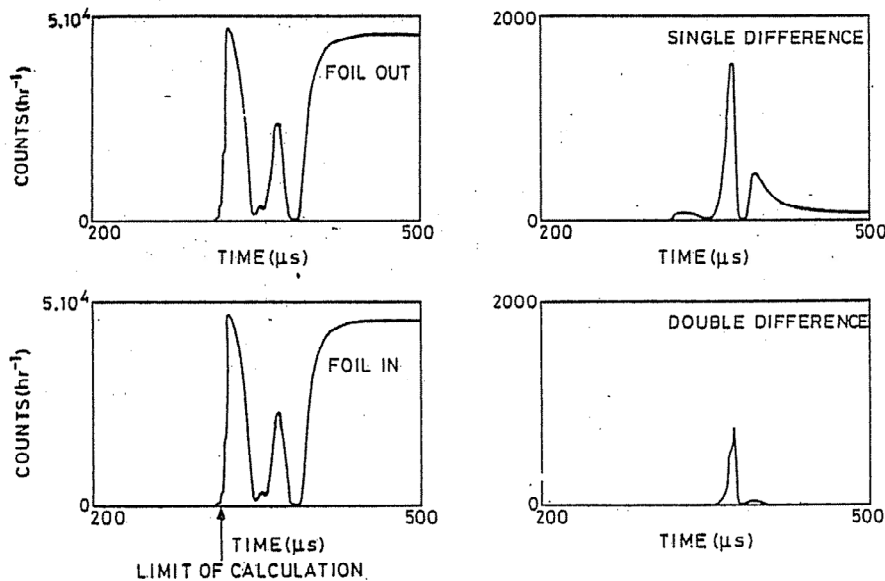


Fig. 13. Simulated TOF spectra for a 25% zirconium hydride scatterer on the prototype eVS at full SNS intensity ($\phi = 5^\circ$); tantalum analyser.

methods; the improved resolution of the latter is self-evident. The parameters used in these calculations are those given in section 6, as relevant to a prototype spectrometer designed for the SNS. We have assumed that the solid angle available in the detector bank is 0.008 sr. We further assumed the sample to be a 25% scatterer and used detection efficiencies appropriate for 10 atm ^3He detectors.

7. Feasibility tests

Experimental tests of the resonance analyser difference method were carried out on the SNS spectrometer LAD [22] which is currently in operation at the Harwell Electron Linac HELIOS. In addition to measuring the inelastic difference scattering it has been possible to assess the effect of diffraction from the analysing foil when it is placed in the incident beam after its transmission through the scatterer. LAD is a total scattering spectrometer and has convenient neutron flight paths ($L_1 = 10.5$ m, $L_2 = 1.0$ m) and detector angles ($\pm 5^\circ$, $\pm 10^\circ$, $\pm 20^\circ$). The detector apertures used were the maximum sizes available: 20×120 mm² at 5° and 10° , 20×250 mm² at 20° . In the limited time available it was only possible to examine briefly the performance of a Sm ($E_R = 0.872$ eV) analyser with a 25% scattering sample of zirconium hydride powder.

The raw TOF and difference spectra for the 5° scattering angle are shown in fig. 14. The fundamental mode is clearly observed and the variation of peak intensity in comparison with the higher scattering angle

results gave the expected Q -dependence. These preliminary results clearly demonstrate the feasibility of the method.

These measurements were originally made with the intention of applying the double difference technique though this did not prove to be possible. It is clear from the single difference TOF spectra that there are significant difference counts in the region of the elastic peak (i.e. at a total time of flight $t \sim 890$ μs), however these are not expected as the simulation given in fig. 12 (where the instrument geometries are very similar) shows. The difference intensity here is expected to be governed by the transmission function of the incident beam filter and should, therefore, be very small. It is evident that this difference intensity is due to neutrons having incident energies just above the incident filter window being down-scattered by exciting very high order overtones in the sample ($\hbar\omega > 7\hbar\omega_0$), and which are then analysed by the thermal Sm resonance at $E_R \sim 0.0976$ eV. This difference scattering may be eliminated by placing a cadmium foil around the detectors, though this was not done in the experiments described. The Sm difference spectra simulations shown in figs. 12 and 15b are, in fact, derived with the effect of Cd included. Fig. 15a is the equivalent to fig. 15b, but without Cd in front of the detector. It may seem surprising that such large energy transfers ($E > 1$ eV) should produce measurable difference count rates, however we should recall that: (1) the thermal Sm resonance has a peak attenuation $\sim 95\%$ in comparison to 60% for the 0.872 eV resonance (and the thin foil thickness), (2) the ^3He detector efficiencies are twice as great at ~ 0.1 eV as at ~ 0.9 eV

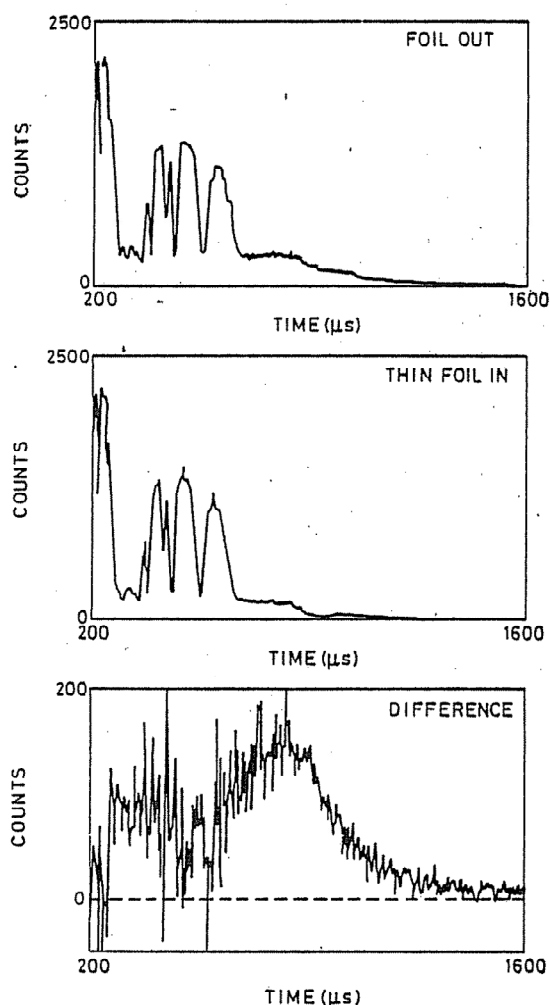


Fig. 14. Raw TOF data for a 25% zirconium hydride scatterer on LAD ($\phi = 5^\circ$, $\Omega/4\pi = 4 \times 10^{-4}$ sr).

and (3) the peak strengths of Einstein oscillators increase with Q and therefore with decreasing analyser energy at fixed scattering angles.

The difference time-of-flight spectrum illustrated in fig. 14 demonstrates that, within the statistical accuracies of these measurements, no diffraction effects from the Sm analyser are observed. Analyser diffraction would give negative difference counts which would also be strongly Q (or detector angle) dependent. The difference spectra observed at $\phi = 10^\circ$ and 20° were not significantly different to the results at 5° . The absence of analyser foil diffraction effects was confirmed in a separate direct diffraction experiment, where the fixed filters were removed and a substantial Sm foil (approximately 5 times thicker than the foil used in these inelastic experiments) was used as the scatterer. The observed spectra at all scattering angles were essentially

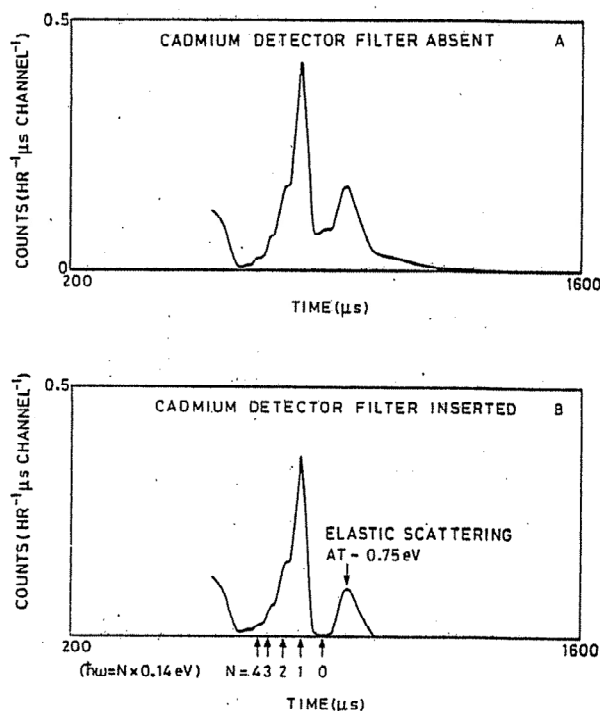


Fig. 15. Effect of thermal samarium resonance: simulated spectra for zirconium hydride on LAD ($\phi = 5^\circ$).

featureless in the time-of-flight region pertinent to the inelastic measurements.

The data presented in this section were collected in approximately three days on a relatively weak pulsed neutron source: the SNS is projected to have approximately 600 times the intensity available from the Harwell Linac during the period of these measurements. Nevertheless it was just possible to observe the fundamental frequency hydrogen vibrations in ZrH_2 , where the double differential cross-section is calculated to be about $3 \text{ b sr}^{-1} \text{ eV}^{-1} \text{ atom}^{-1}$. This cross-section is relatively large compared to those associated with electronic transitions, though with the more powerful sources it is expected that the technique described here would allow the study of mixed valence systems [23] which have cross-sections $\sim 0.1\text{--}0.3 \text{ b sr}^{-1} \text{ eV}^{-1}$, paramagnetic metals [24] which have estimated cross-sections $1 \text{ mb sr}^{-1} \text{ eV}^{-1}$, and Stoner excitations [25] which have cross-sections $\sim 1\text{--}3 \text{ mb sr}^{-1} \text{ eV}^{-1}$.

8. Summary

The principle of the resonance absorption filtered beam difference method in the inverse geometry has been described and a design for a suitable spectrometer presented. The feasibility of the technique has been

demonstrated in experiments on ZrH_2 . It was concluded that it should be possible to use it to examine many magnetic and electronic excitations in the eV region requiring low Q which have hitherto been inaccessible; this is particularly the case with the advent of the most powerful of the new generation of pulsed neutron sources such as the SNS.

The authors would like to thank colleagues at RAL, Harwell and at the WNR and IPNS facilities for their contributions and comments. Thanks are also due to the Neutron Groups at Los Alamos for their hospitality during the period in which this paper was drafted.

References

- [1] S.K. Sinha, *J. Appl. Phys.* 50 (1979) 1952.
- [2] J.F. Cooke and J.A. Blackman, *Phys. Rev.* B26 (1982) 4410.
- [3] D.R. Allen, E.W.J. Mitchell and R.N. Sinclair, *J. Phys.* E13 (1980) 639.
- [4] R.N. Sinclair, M.C. Moxon and J.M. Carpenter, *Bull. Am. Phys. Soc.* 22 (1977) 101.
- [5] L. Cser, N. Kroo, P. Pacher, V.G. Simkin and E.V. Vasilyeva, *Nucl. Instr. and Meth.* 179 (1981) 515.
- [6] J.M. Carpenter, N. Watanabe, S. Ikeda, Y. Masuda and S. Sato, to be published in *Nucl. Instr. and Meth.*
- [7] R.M. Brugger, A.D. Taylor, C.E. Olsen, J.A. Goldstone and A.K. Soper, *Proc. 6th Int. Collaboration on Advanced neutron sources (ICANS-VI)*, Argonne National Laboratory (1982).
- [8] W.G. Williams and J. Penfold, *ibid.*
- [9] R.J. Newport and W.G. Williams, Rutherford Appleton Laboratory Report RL-83-052 (1983).
- [10] P. Seeger, A.D. Taylor and R.M. Brugger, to be published.
- [11] A.D. Taylor, R.A. Robinson and P. Seeger, Los Alamos Laboratory Report LAUR 83-1499 (1983) and to be published in *Nucl. Instr. and Meth.*
- [12] R.M. Richardson, Rutherford Appleton Laboratory Report RL-82-035 (1981).
- [13] D.J. Hughes, *Neutron cross sections* (Pergamon, London, 1957).
- [14] J.M. Blatt and V.F. Weisskopf, *Theoretical nuclear physics* (Springer New York, 1952).
- [15] A. Foderaro, *The elements of neutron interaction theory* (MIT Press, 1971).
- [16] F.F. Freeman and W.G. Williams, *J. Phys.* E11 (1978) 459.
- [17] T. Springer, *Quasielastic neutron scattering*, Springer tracts in modern physics vol. 64 (Springer, Berlin, 1972).
- [18] B.H. Meardon, Rutherford Laboratory Report RL-74-144 (1974).
- [19] C.G. Windsor, *Pulsed neutron scattering* (Taylor and Francis, London, 1982).
- [20] D.F.R. Mildner, B.C. Boland, R.N. Sinclair, C.G. Windsor, L.J. Bunce and J.H. Clarke, *Nucl. Instr. and Meth.* 152 (1978) 437.
- [21] B.C. Boland, D.F.R. Mildner, G.C. Stirling, L.J. Bunce, R.N. Sinclair and C.G. Windsor, *Nucl. Instr. and Meth.* 154 (1978) 349.
- [22] W.S. Howells, Rutherford Laboratory Report RL-82-035 (1982).
- [23] S.M. Shapiro, R.J. Birgenau and E. Bucher, *Phys. Rev. Lett.* 34 (1975) 470.
- [24] S. Doniach, *Proc. Phys. Soc.* 91 (1967) 813.
- [25] R.D. Lowde and C.G. Windsor, *Adv. Phys.* 19 (1970) 813.